Available online at www.sciencedirect.com
SCIENCE DIRECT
Remote Sensing of Environment 101 (2006) 150 – 166
Remote Sensing of Environment
www.elsevier.com/locate/rse

Estimating the probability of mountain pine beetle red-attack damage

M.A. Wulder [a,*], J.C. White [a], B. Bentz [b], M.F. Alvarez [c], N.C. Coops [d]

[a] Canadian Forest Service, Pacific Forestry Centre, 506 West Burnside Road, Victoria, British Columbia, Canada, V8Z 1M5
[b] United States Department of Agriculture, Forest Service, Rocky Mountain Research Station, 860 N. 1200 E., Logan, UT 84321, USA
[c] Universidad de León, E.S.T. Ingeniería de Minas, Avd. Astorga s/n 24400, Ponferrada, Leon, Spain
[d] Department of Forest Resource Management, 2424 Main Mall, University of British Columbia, Vancouver, British Columbia, Canada, V6T 1Z4

Received 27 September 2005; received in revised form 7 December 2005; accepted 10 December 2005

Abstract

Accurate spatial information on the location and extent of mountain pine beetle infestation is critical for the planning of mitigation and treatment activities. Areas of mixed forest and variable terrain present unique challenges for the detection and mapping of mountain pine beetle red-attack damage, as red-attack has a more heterogeneous distribution under these conditions. In this study, mountain pine beetle red-attack damage was detected and mapped using a logistic regression approach with a forward stepwise selection process and a set of calibration data representing samples of red-attack and non-attack from the study area. Variables that were considered for inclusion in the model were the enhanced wetness difference index (EWDI) derived from a time series of Landsat remotely sensed imagery, elevation, slope, and solar radiation (direct, diffuse, and global). The output from the logistic regression was a continuous probability surface, which indicated the likelihood of red-attack damage. Independent validation data were used to assess the accuracy of the resulting models. The final model predicted red-attack damage with an accuracy of 86%. These results indicate that for this particular site, with mixed forest stands and variable terrain, remotely sensed and ancillary spatial data can be combined, through logistic regression, to create a mountain pine beetle red-attack likelihood surface that accurately identifies damaged forest stands. The use of a probabilistic approach reduces dependence upon the definition of change by the application of thresholds (upper and lower bounds of change) at the image processing stage. Rather, a change layer is generated that may be interpreted liberally or conservatively, depending on the information needs of the end user.

Keywords: Forest; Mountain pine beetle; Logistic regression; Landsat; Tasseled cap; Change detection

1. Introduction

When mountain pine beetle populations reach epidemic levels, they generally spread through mature pine stands, potentially resulting in extensive mortality of large-diameter trees. Virtually all species of pine within the mountain pine beetle's range, are suitable hosts (Furniss & Schenk, 1969; Smith et al., 1981); however, due to the size, intensity, and the commercial impact of epidemics, lodgepole pine (*Pinus contorta* Dougl. ex Loud. var. *latifolia* Engelm.) is the species most severely impacted by the beetle and, therefore, is considered the mountain pine beetle's primary host. Native to North America, the mountain pine beetle's current biological range is believed to extend from northern British Columbia and western Alberta south to northwestern Mexico, and from the Pacific Coast eastward to the Black Hills of South Dakota. Suitable habitat for the beetle has been found at elevations ranging from sea level in British Columbia to 3353 m in southern California (Amman et al., 1989).

The impact of mountain pine beetle is evident throughout its biological range. In the United States, the area affected by the beetle increased from a total of approximately 156,090 ha in 1999 to 898,040 ha in 2003. In British Columbia, the mountain pine beetle population has reached epidemic levels, with the area of infested forest increasing from approximately 164,000 ha in 1999 to 7,089,900 ha in 2004 (Westfall, 2005). The biological range of the primary host, lodgepole pine, exceeds the current range of the mountain pine beetle; however, recent research has indicated that the beetle is expanding into new geographic areas with the range expansion believed to be related to changes in

* Corresponding author. Tel.: +1 250 363 6090; fax: +1 250 363 0775.
E-mail address: mwulder@nrcan.gc.ca (M.A. Wulder).

0034-4257/$ - see front matter © 2006 Elsevier Inc. All rights reserved.
doi:10.1016/j.rse.2005.12.010

climate (Carroll et al., 2004; Logan & Powell, 2004). The two factors that have contributed to the successful expansion of the beetle population in British Columbia include the large amount of mature lodgepole pine on the land base, which has tripled in the last century as a result of intensive fire suppression activities (Taylor & Carroll, 2004), and several successive years of favorable climate conditions, resulting in an increase in suitable areas for brood development and success (Carroll et al., 2004).

The phenology of the mountain pine beetle and the associated host response have implications for the timing at which surveys of beetle damage are undertaken. In general, mountain pine beetles in British Columbia produce a single generation per year (Carroll & Safranyik, 2004; Safranyik et al., 1974). Adult beetles typically attack trees in August and lay eggs, which complete their development cycle into mature adults approximately 1 year later (Amman & Cole, 1983). The mountain pine beetle uses two tactics to overcome the defenses of a healthy tree. First, the beetles may attack in large numbers through a cooperative behaviour termed as a mass attack. By rapidly concentrating their attack on selected trees, the beetles are capable of exhausting the host's defensive response (Berryman, 1976; Berryman et al., 1989; Raffa & Berryman, 1983; Safranyik et al., 1974). Secondly, the beetles have a close association with several microorganisms, which the beetles carry into the tree with them when they attack. In particular, the spores of two blue stain fungi (*Ophiostoma clavigerum* and *Ophiostoma montium*) are inoculated into the tree as the beetles bore through the tree's bark. These fungal spores penetrate living cells in the phloem and xylem (Ballard et al., 1982, 1984; Safranyik et al., 1975; Solheim, 1995), resulting in desiccation and disruption of transpiration (Mathre, 1964), effectively stopping resin production by the tree (Carroll & Safranyik, 2004).

Immediately following a mass attack, the foliage of trees remains visibly unchanged; however, a drop in sapwood moisture has been measured as a consequence of the attack (Reid, 1961; Yamaoka et al., 1990). Once the tree is killed, but still with green foliage, the host tree is in the green-attack stage. The first visible sign of impact is a change in foliage colour from green to greenish-yellow that usually begins in the top of the crown. These trees are referred to as faders. Generally, the foliage fades from green to yellow to red over the spring and summer following attack (Amman, 1982; Henigman et al., 1999). The leaves gradually desiccate and the pigment molecules break down; initially the green chlorophyll pigment molecules are lost, then the yellow carotenes and red anthocyanins (Hill et al., 1967). Slowly, the needles drop until the tree is completely defoliated. Twelve months after being attacked over 90% of the killed trees will have red needles (red-attack). Three years after being attacked, most trees will have lost all needles (gray-attack) (British Columbia Ministry of Forests, 1995). There is variability associated with the progression of attack stages; the rate at which the foliage will discolour varies by species and by site (Safranyik, 2004).

Mountain pine beetle success at higher elevations has typically been considered limited due to a lack of sufficient thermal energy to complete the life cycle in a single year (Amman, 1973). A univoltine (single brood per year) life cycle is considered a basic requirement to maintaining an appropriate seasonality and therefore population success (Amman, 1973; Logan & Bentz, 1999; Safranyik, 1978). However, increasing temperatures observed in the past 5 to 10 years may be nullifying the effect of elevation, as successful univoltine mountain pine beetle populations are currently being observed in pine ecosystems as high as 3000 m (Logan & Powell, 2001). In areas with more extreme topographic relief and where conditions are considered marginal for the establishment of a mountain pine beetle population (Amman, 1973; Logan & Powell, 2001), topographic attributes such as elevation, slope, and solar radiation may have a stronger influence on the efficacy of beetle infestations.

The infrared and short-wave infrared channels of the Landsat sensor are known to be particularly sensitive to changes in forest structural changes (Horler & Ahern, 1986). Image transformations that exploit changes over time in the infrared and short-wave infrared channels have shown success in mapping subtle forest changes resulting from insect disturbance (Price & Jakubauskas 1998), through to stand replacing disturbances such as harvests (Cohen et al., 1995). Single date mapping of red-attack is based upon the contrast in attacked stands in relation to non-attack stands. While reasonable classification accuracies may be found (73.3%±6.7%, $\alpha=0.05$) issues with omission and commission error may emerge (Franklin et al., 2003). To address limitations related to mapping a change feature with single date imagery, change detection approaches were developed and applied. Following examples in the literature illustrating the strength of approaches based upon the tasselled cap transformation (TCT) for capturing change, the Enhanced Wetness Difference Index (EWDI) was developed (Franklin et al., 2000, 2001). The Skakun et al. (2003) approach is based upon the application of a user defined threshold to the differences found between a spectral index generated from two dates of imagery. The results of this type of threshold based approach are products that are binary in nature, with pixels identified as either having red-attack damage, or not having red-attack damage. Attribute specific red-attack accuracy ($\alpha=0.05$) ranged from 76% to 81% (as stratified by level of attack: for groups of 10–29 red-attack trees=76%±12%, and for groups of 30–50 red-attack trees=81%±11%) (Skakun et al., 2003).

The objectives of the research conducted for this paper were two-fold. The first objective was to build on past research undertaken by Skakun et al. (2003), by using a logistic regression approach to generate products indicating a range of red-attack likelihood, rather than a binary indication of red-attack and non-attack. The second objective was to capitalize upon the opportunity afforded by using a logistic regression based approach to include additional spatial information layers in the mapping algorithm. Rather than a disturbance feature mapping approach based solely upon remotely sensed data, we explore the influence of topographic and solar radiation variables on the estimation of red-attack damage in an area of mixed forest and variable terrain.

2. Study area

Located in Western Montana, the Lolo National Forest contains a highly diverse range of forest ecosystems (Fig. 1) and is mountainous, with elevations ranging from 940 to 1524 m. The dominant forest type in the area is mixed conifer, which includes subalpine fir (*Abies lasiocarpa*), mountain hemlock (*Tsuga mertensiana*), western hemlock (*Tsuga heterophylla*), larch (*Larix occidentalis*), grand fir (*A. grandis*), Douglas-fir (*Pseudotsuga menziesii*), and lodgepole pine (*Pinus contorta*). The current forest inventory (circa 2004), indicates that the dominant single species, by area, is Douglas-fir (47% of the study area), followed by lodgepole pine (16% of the study area). Aerial overview surveys indicate that the mountain pine beetle first appeared in this area in 1994. In 2004, the area had 4500 ha of trees killed by mountain pine beetle (mostly lodgepole pine). The study area has experienced an unprecedented 7-year period of drought, and prolonged drought has been shown to contribute to the increased susceptibility of pine forests to attack by mountain pine beetle (Safranyik, 2004; Safranyik et al., 1975). The spatial nature of the mountain pine beetle population within the region is characterized by small and widely scattered groups of red- and gray-attack trees. Locations of red-attack damage in 2001, 2002, and 2003, as identified in the aerial overview survey data, are shown in Fig. 2.

3. Data and methods

3.1. Ground surveys to identify forest stands with red-attack damage

Although the forest conditions within the study area were mixed conifer, field measurements, which were collected annually from 1999 to 2002, were restricted to areas dominated by lodgepole pine. The objective of this study was to use the Landsat imagery to detect and map mountain pine beetle red-

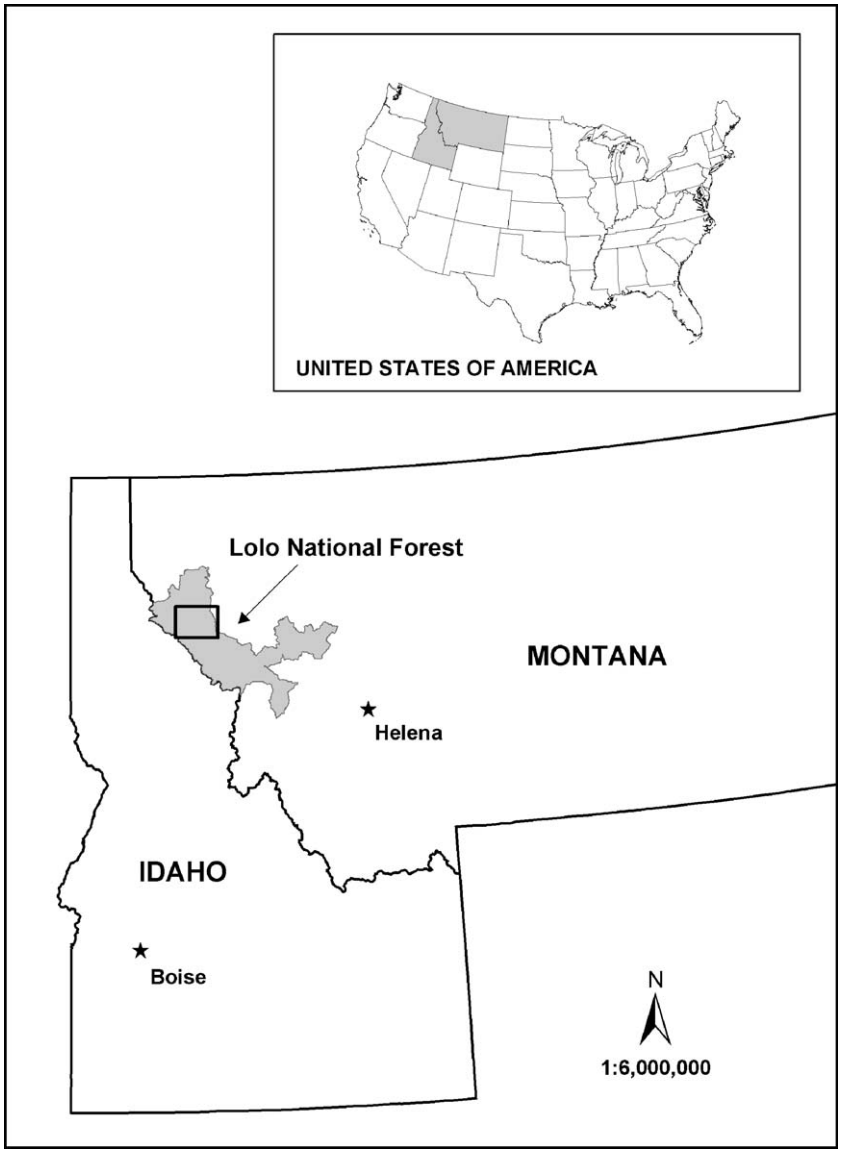

Fig. 1. Location of the study area in the Lolo National Forest.

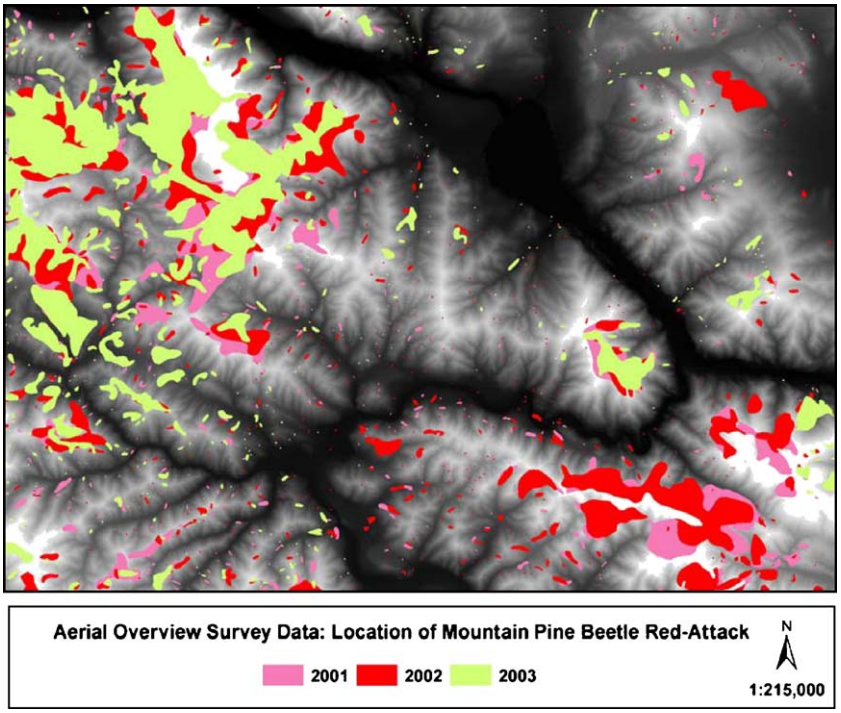

Fig. 2. Aerial overview survey data for the study area collected in 2001, 2002, and 2003.

attack trees in 2002, hence field measures of red-attack damage collected during the months of August and September in both 2001 and 2002, were used.

A total of 13 and 30 plots were established in 2001 and 2002, respectively. In both years, each plot consisted of a grid of 30 m × 30 m (0.09 ha) sub plots, either 3 × 3 in 2001 or 2 × 2 in 2002, resulting in 117 sub plots in 2001 and 120 in 2002. The sampling intensity was altered in 2002 to facilitate an increase in the number of sites across the area. In all cases the plots were oriented in a north–south direction, diameter at breast height (dbh) was measured for all trees, with each tree assigned a species and attack code, as indicated in Table 1. The attack code was determined by examining the tree for evidence of mountain pine beetle. This evidence includes the presence of pitch tubes and/or boring dust around the base of the tree, as well as beetle galleries and developing brood under the bark of the tree (Safranyik et al., 1975). In addition, the colour of the tree crown is examined and recorded. The colour of the crown, combined with evidence of beetle activity determines which of the five codes are assigned to the tree.

The location information of each site was verified by locating the plot coordinates in a Geographic Information System (GIS) and comparing the location (using imagery and planimetric base maps) to the detailed sketch maps drawn by the field crews at each plot. Of the 237 plots available, two sites (16 plots) were dropped due to errors in positioning, leaving 213 plots remaining.

Since the objective was to identify red-attack trees in 2002 and the infestation in this area had been on-going for a number of years, we chose to stratify the 213 plots by the presence of red-attack crowns in the stand, and then further stratify these plots by the percentage of gray-attack trees. Based on the mountain pine beetle life cycle, plots with a presence of a gray-attack trees must have first been attacked either in, or prior to, 1999. As a result, the selection of ground survey plots for use as calibration or validation data was restricted to those plots that had less than 25% gray-attack. This resulted in a reduced sample of 136 plots. From this sample, approximately half of the plots were randomly selected for calibration of the classification algorithm and the other half were retained as independent validation data. Distributions of the variables in the two data sets were examined to ensure that each were similar for attributes of interest, such as percent gray-attack, elevation, slope, and solar radiation. The spatial distribution of the ground plots is presented in Fig. 3.

Table 1
Codes assigned to ground samples

Code	Description
1	Live and not currently infested
2	Current mountain pine beetle attack
3	Attacked previous year
4	Attacked 2 years previous
5	Attacked more than 2 years previous

3.2. Landsat ETM+ imagery

Landsat 7 ETM+ imagery were acquired for August 26, 1999 and August 18, 2002. The 1999 image was geometrically rectified to Universal Transverse Mercator (UTM), Zone 11 N, North American Datum 1927 using planimetric base data. The 2002 image was geometrically registered to the 1999 image with a root mean square error of less than 0.4 pixel using 26 ground control points, a second-order polynomial transformation, and nearest neighbour interpolation. A top-of-atmosphere

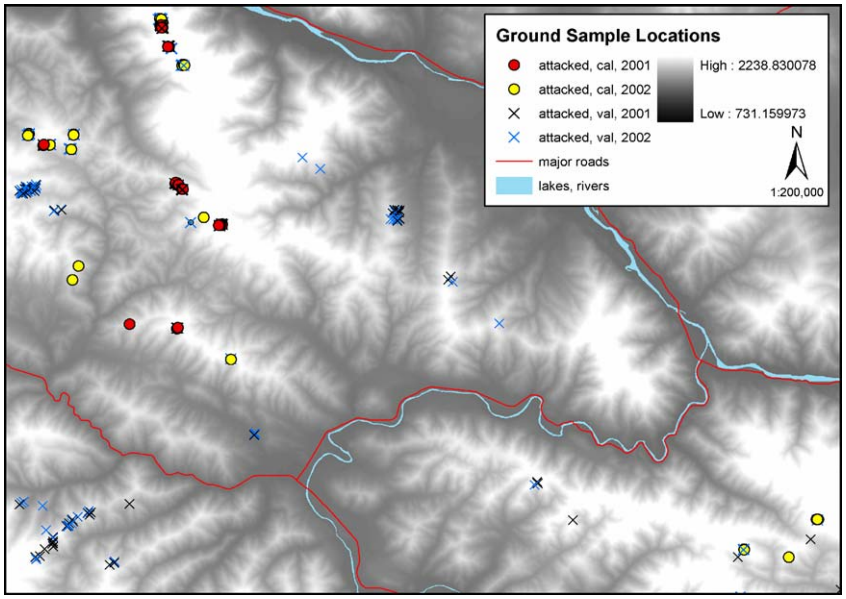

Fig. 3. Distribution of ground samples across the study area.

(TOA) correction was applied to both image dates to convert them to TOA reflectance (Markham & Barker, 1986). This correction accounts for differences in sensor and viewing geometry, but does not correct for variations in absolute atmospheric conditions between images.

3.3. Image analysis to identify non-attacked forest stands

A sample of non-attacked trees was required for the classification procedure and for validation; without these data, errors of commission and omission associated with the detection of red-attack damage could not be characterized (Wulder et al., 2004). However, the ground survey did not collect any data for plots that were not attacked. This lack of field data combined with the retrospective nature of the analysis (using 1999 and 2002 imagery) confounded efforts to obtain calibration and validation data for the non-attack class. In the absence of aerial photography or other suitable high spatial resolution data (collected at the same time as the Landsat data), an image based source of calibration and validation data was considered the best alternative. A sample of non-attacked stands was therefore generated by calculating the greenness component of the Tasselled Cap Transformation (TCT) for the 2002 Landsat image using coefficients developed Huang et al. (2002). The greenness component of the TCT indicates the abundance and vigour of the vegetation cover (Crist & Kauth, 1986; Dymond et al., 2002; Gong et al., 2003; Healy et al., 2005), and is designed to be orthogonal from the other TCT components. To assess this, the correlation between TCT greenness and wetness values in areas dominated by lodgepole pine was tested. For the 2002 Landsat 7 ETM+ image, the mean wetness value was −19.36 (SD=18.78) and the mean greenness value was 15.36 (SD=10.97). Pearson's correlation supports the hypothesis that there is no significant correlation between wetness and greenness TCT components for 2002 ($r_{(914095)}=0.1204$, $p<0.05$). The assumption was made that pixels having high greenness values would be less likely to contain large numbers of red-attack trees.

A mask was generated from the forest inventory, which included all of the forest stands that had pine as the leading species. All of the greenness values located under this pine mask were extracted and sorted by magnitude; the largest 1000 greenness values were retained and a random sample of 136 values was selected. To ensure that the sample was representative of forest conditions captured at the red-attack sample locations, the mean crown closures for the red-attack and non-attack samples were tested and found to not be significantly different (as determined using a two-sided t-test, $t_{(161)}=1.97$, $p=0.87$). The result of the image analysis described above is a representative sample of non-attack pixels in those areas of the study site dominated by lodgepole pine, which complements the sample of red-attack pixels collected. Half of the non-attacked sample was randomly selected for calibration, and half were retained as independent validation data.

3.4. Enhanced wetness difference index

The Tasseled Cap Transformation is a reduction in the six reflectance channels of a single date of Landsat imagery to three components: brightness, greenness, and wetness (Crist & Cicone, 1984; Crist et al., 1986; Kauth & Thomas, 1976). The wetness component of the TCT is generated for each of the images using the following equation (Huang et al., 2002):

$$\begin{aligned}\text{Wetness} = {} & 0.2626(\text{ETM}+1) + 0.2141(\text{ETM}+2) \\ & + 0.0926(\text{ETM}+3) + 0.0656(\text{ETM}+4) \\ & - 0.7629(\text{ETM}+5) - 0.5388(\text{ETM}+7) \end{aligned} \quad (1)$$

where ETM+N=Enhanced Thematic Mapper Band N.

The term "Enhanced Wetness Difference Index" or EWDI, was first used by Franklin et al. (2000). In this study, visual interpretation of change between 1997 and 1998 was facilitated by displaying the TCT wetness component for 1998 through the green and blue colour guns of the display, while the TCT wetness component for 1997 was displayed through the red colour gun of the display. A linear stretch was applied to increase contrast. The result is an image in the display where a decrease in wetness from 1997 to 1998 is depicted in various shades of red; an increase in wetness from 1997 to 1998 is depicted in various shades of blue/green; and no change between the 2 years is depicted in white. An example of this display for the Lolo study area is provided in Fig. 4. Although the wetness index values used for analysis and thresholding are derived by subtracting the TCT wetness component for 1 year from the TCT wetness component for a second year, the term EWDI has persisted in studies subsequent to Franklin et al. (2001), including those where visual interpretation of change was not the method used to identify change (e.g., Franklin et al., 2002, 2003, 2005; Skakun et al., 2003; Wulder et al., 2005). The wetness index approach used in this paper builds on past work by Franklin et al. (2003) and Skakun et al. (2003). The EWDI has been demonstrated as an effective means for detecting red-attack damage. Cohen et al. (2003) characterize the advantages of incorporating multiple dates of imagery to strengthen regression models; however, they emphasize the utility of integrating these multiple dates into a single index for regression modeling. This is the approach applied in this analysis.

The EWDI is generated by subtracting the wetness values from the most recent image date (T2) from the wetness values from the older image date (T1). Therefore:

$$\mathrm{EWDI} = \mathrm{T1} - \mathrm{T2} \quad (2)$$

Areas where moisture has decreased from year T1 to year T2 will generally have positive EWDI values. Conversely, areas where moisture has increased from year T1 to year T2 will generally have negative values. Areas where there is no change in moisture will typically have EWDI values close to zero. The magnitude of the positive or negative EWDI values is indicative of the magnitude of the moisture difference between the two image dates. Fig. 5 shows an example of the distribution of EWDI values for forest that is not attacked versus EWDI values for forest with red-attack damage. Change in the wetness values between the two dates is a general indicator of conifer mortality; the wetness component captures the mid-infrared changes and is considered the most consistent single indicator of forest change (Collins & Woodcock, 1996).

3.5. Digital elevation model

Digital elevation data of the area was produced by the United States Geological Survey as part of the National Elevation Dataset (NED) using 1:60,000 photography, and resulting in a seamless mosaic digital elevation model (DEM) at 30 m spatial resolution (United States Geological Survey, 1999). A key feature of the NED DEM is the comprehensive pre-processing procedures, which reduce errors and facilitate the calculation of derivatives such as slope; slope was

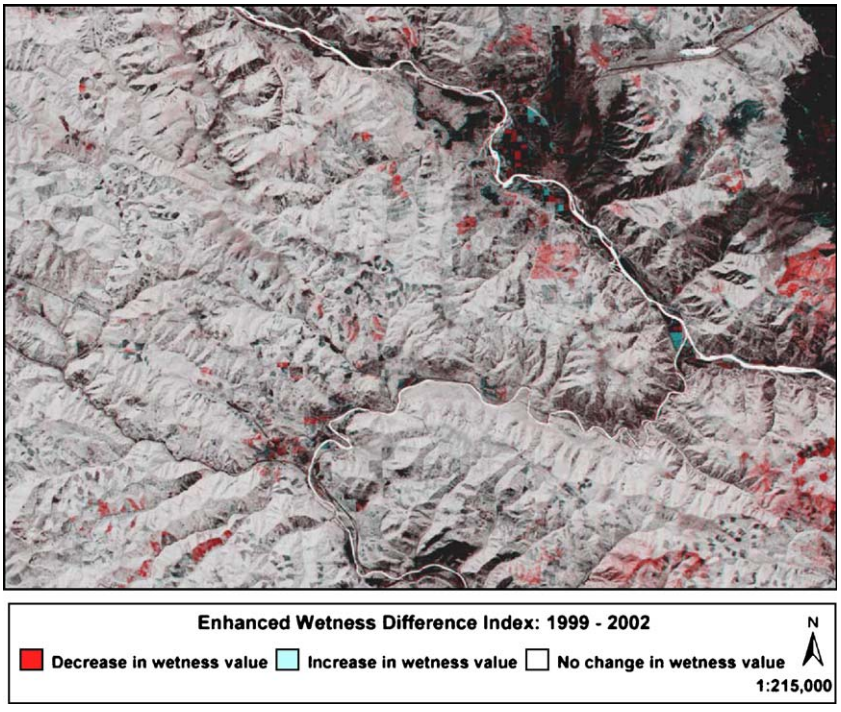

Fig. 4. The enhanced wetness difference index (EWDI). Areas in red indicate decreases in moisture between the two image dates (1999 and 2002), while blue areas indicate increases in moisture and white areas indicate no change. (For interpretation of the references to colour in this figure legend, the reader is referred to the web version of this article).

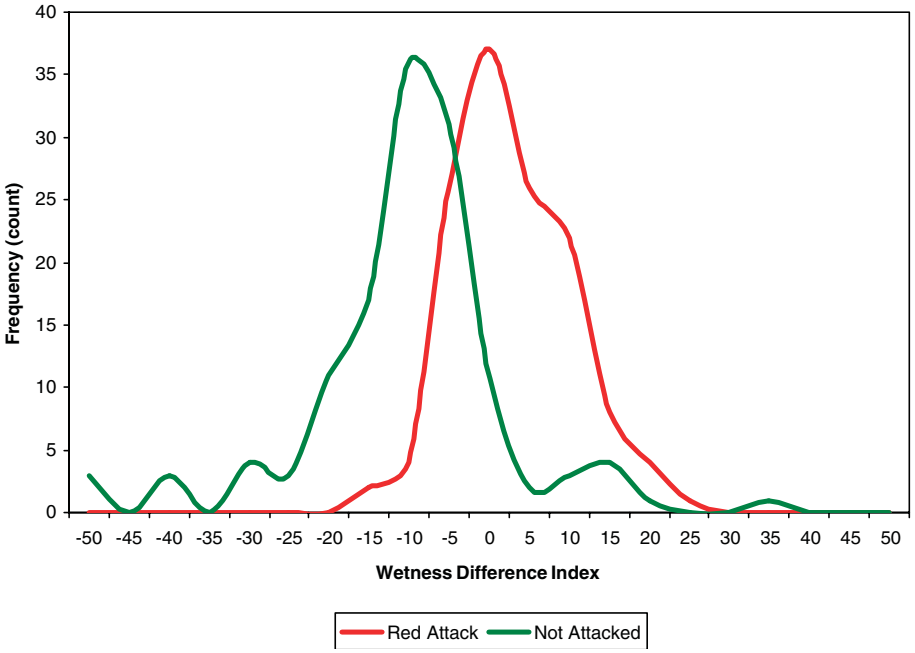

Fig. 5. Distribution of enhanced wetness index values for both red-attack (red) and non-attack samples (green). (For interpretation of the references to colour in this figure legend, the reader is referred to the web version of this article).

estimated within a window of 3×3 cells using the average maximum technique (Burrough, 1986; Oksanen & Sarjakoski, 2005).

3.6. Solar radiation

Direct clear-sky solar radiation was calculated using the equation developed by Kreith and Kreider (1978) and implemented using a process developed by Kumar et al. (1997). Direct solar radiation is defined as the radiation received directly on a horizontal surface, without any absorption or scattering. Diffuse solar radiation is defined as that portion of the solar radiation that is scattered downwards by the molecules in the atmosphere. Diffuse solar radiation varies between summer and winter and is a function of solar altitude and terrain reflectance. Global solar radiation is calculated by summing direct and diffuse solar radiation. Solar radiation and related variables can aid in the prediction of vegetation type and growth (Franklin, 1995). Kumar et al. (1997) provide scripts (coded in Arc Macro Language), which use a DEM as input to calculate short-wave direct and diffuse radiation received at the surface of the earth over a specified period of time.

3.7. Logistic regression model

The discrete nature of the dependent variable (i.e., red-attack, non-attack) was well suited to the use of logistic regression. Logistic regression has become a widely used and accepted method of analysis of binary outcome variables as it is flexible and predicts the probability for the state of a dichotomous variable (i.e., red-attack, non-attack) based on predictor variables (e.g. EWDI, slope, solar radiation) and has widely been applied in forestry to estimate tree and stand survival under competition (e.g., Monserud, 1976; Monserud & Sterba, 1999; Shen et al., 2000; Yao et al., 2001; Vanclay, 1995). In the field of remote sensing, logistic regression has been used for land cover change detection (e.g., Fraser et al., 2003, 2005) and for mapping insect tree defoliation (Ardö et al., 1997; Fraser & Latifovic, 2005; Lambert et al., 1995; Magnussen et al., 2004). Lambert et al. (1995) used dichotomous logit regression to discriminate among three defoliation categories of Norway spruce in the Czech Republic using Landsat TM imagery, with accuracies ranging from 76% to 88%. Magnussen et al. (2004) developed a logistic regression model for spatially explicit predictions of the likelihood of an onset of stand-level spruce budworm (*Choristoneura fumiferana*) defoliation.

Table 2
Parameters and fit statistics for the logistic regression model with only EWDI as predictor of red-attack damage

Model parameters		Wald test		Nagelkerke's R^2	Hosmer and Lemeshow's goodness of fit test	
Parameter	α_i	Wald	Sig.	R^2	Chi-square	Sig.
Intercept	0.763748701	8.281	0.004	0.454	26.085	0.001
EWDI	0.160302107	28.578	0.000	$p = \frac{1}{1 + e^{-(\alpha_0 + \alpha_2 \text{EWDI})}}$		
	$e^{\beta} = 1.17386545$ percent chg. in odds = 17.38%					

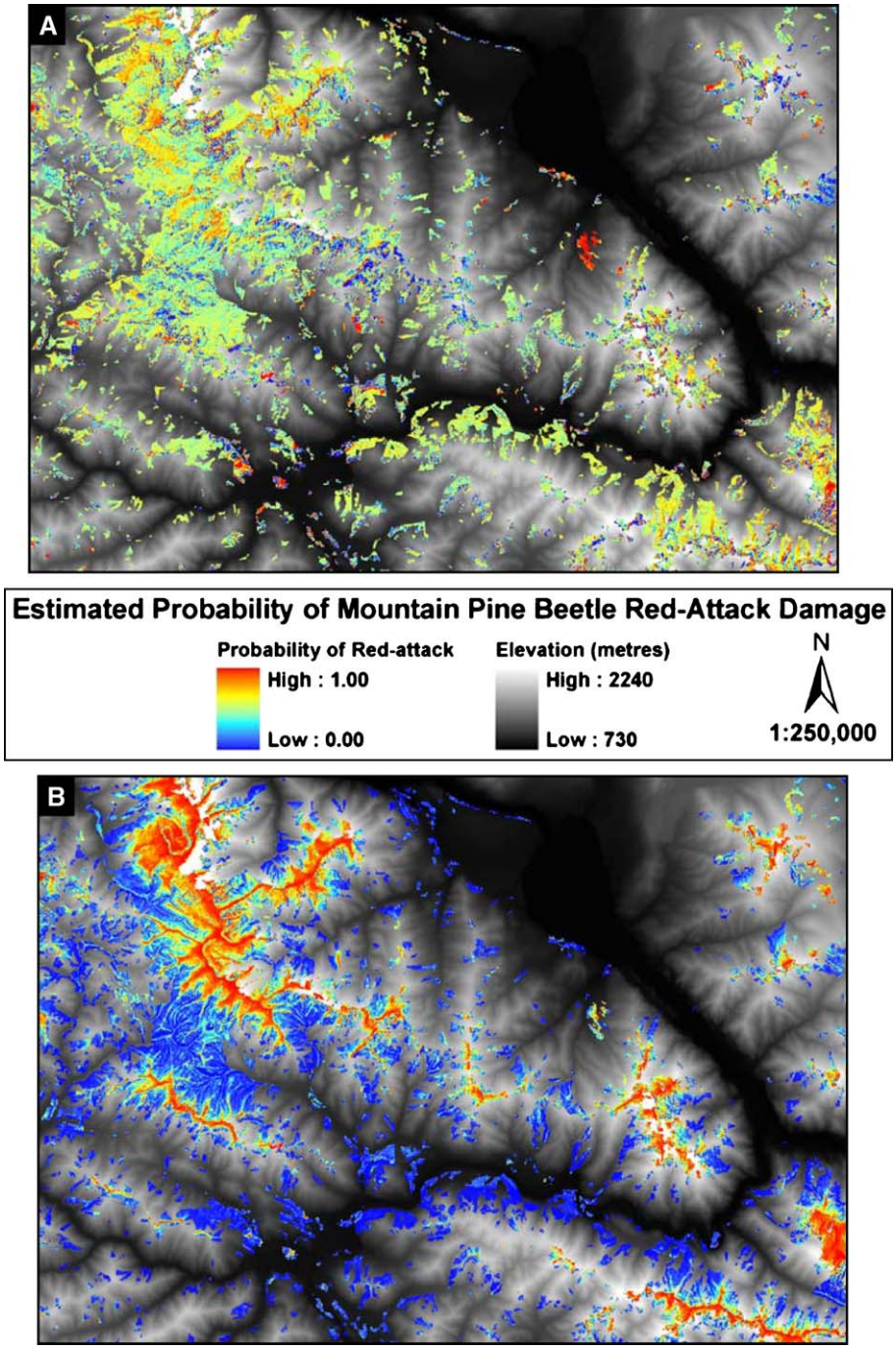

Fig. 6. Output of logistic regression model using (A) EWDI only and (B) EWDI with elevation and slope.

The logistic regression model presented here has a dependent variable that is transformed into a logit variable, calculated as the neperian logarithm (ln) of the probability of a certain event occurring (p) divided by the probability of no event ($q=1-p$) (Bergerud, 1996). Then, the linear logistic model is fitted by the method of maximum likelihood, estimating the probability of success for binary response data. Generalized for k independent explanatory variables ($x_1,\ldots,x_k$) the logistic regression model can be presented as in Eq. (3) (Norušis, 2005):

$$\ln(p/q) = \alpha_0 + \alpha_1 x_1 + \ldots + \alpha_k x_k \quad (3)$$

where: ln is the neperian logarithm, p the probability of success (i.e., attacked), q the probability of failure ($p+q=1$), α_0 and α_1 are constants, and x_i is a variable which can be continuous or discrete and randomly distributed or not. The model can be also expressed using Eq. (4), which allows straightforward calculation of the probability of the binomial process (i.e., attacked) for different values of the independent variables x_i:

$$p = \frac{1}{1 + e^{-(\alpha_0+\alpha_1 x_1+\ldots+\alpha_k x_k)}} \quad (4)$$

Logistic regression calculates changes in the logit variable, not in the dependent itself, as is the case with ordinary least

Table 3
Results of the validation of the logistic regression model using EWDI for red-attack mapping

Predictor: EWDI		Logistic model			Producer's accuracy	Omission error	
		Non-attack	Red-attack	Total			
Reference data	Non-attack	53	11	64	82.81%	17.19%	
	Red-attack	21	43	64	67.19%	32.81%	
	Total	74	54	128	Overall accuracy		
User's accuracy		71.62%	79.63%		Lower CI	Value	Upper CI
Commission error		28.38%	20.37%		66.82%	75.00%	81.69%

Confidence intervals calculated at 95% confidence coefficient.

squares regression (OLS) (Hosmer & Lemeshow, 2000), which enables the method to overcome many of the restrictive assumptions of OLS regression (Press & Wilson, 1978). As a result, the dependent variable need not be normally distributed, there is no homogeneity of variance assumption, error terms do not need to be normally distributed, and independent variables do not need to be interval or unbounded (Rice, 1994).

The interpretation of a logistic regression coefficient, b, is not as straightforward as that of a linear regression coefficient, and hence the coefficients are often converted into odds ratios by exponentiating the coefficient (Bergerud, 1996; Norušis, 2005). e^{β} represents the ratio-change in the odds of the event of interest (red-attack) for a one-unit change in the predictor. Therefore, e^{β} informs about the amount of change in the odds of being attacked relative to changes in the independent variable, while the sign of the b coefficient indicates whether an increase in one dependent variable involves an increase or a decrease in the probability of a pixel having red-attack damage. To further ease interpretation, the e^{β} may be converted to a percentage change in odds using Eqs. (5) and (6):

$$e^{\beta} = \frac{\text{odds after the change in X}}{\text{odds before the change in X}} \quad (5)$$

$$\left(e^{\beta} - 1\right)*100 \quad (6)$$

The logistic model assumes that all independent variables in the regression model are relevant, the dependent variable is independently and randomly sampled, the probability of the dependent variable is a logit function of the independent variables (Bergerud, 1996), and that there is no multicollinearity and absence of outliers (Rice, 1994). Moreover, large samples are required, because the maximum likelihood estimation (MLE) involves a decline in reliability of estimates when there are few cases for each observed combination of independent variables. Peduzzi et al. (1996) recommend a minimum of 10 observations per parameter in the model.

The linear logistic regression model was fitted and validated using the SPSS™ software (SPSS for Windows, Release 13.0, 2004. Chicago: SPSS Inc.). The convention for binomial logistic regression was followed and the dependent class of greatest interest (i.e., red-attack) was coded as 1, and the another class (i.e., non-attack) as 0. A forward selection method was used to establish the most significant input variables, and the results compared to those obtained by using the backwards selection method. A threshold was set to assign data to each class (red-attack or non-attack) according to the predicted probability value; the selected threshold of 0.5 means that if the probability of belonging to class 1 (red-attack) is higher than 0.5 (50%), that point would be assigned to the red-attack class.

3.8. Model validation

Model validation was performed calculating fit statistics and prediction errors (Tables 2 and 4). Strength of association was assessed by the Nagelkerke's R-Square (R^2), which is a further modification of the Cox and Snell coefficient so that it varies between 0 to 1 (Nagelkerke, 1991). It can be interpreted in a similar way to the OLS multiple R^2, although it usually reaches lower values and it is based on likelihood (Norušis, 2005). The Hosmer and Lemeshow's Goodness of Fit Test (Hosmer & Lemeshow, 2000) tests the null hypothesis that the data were generated by the model fitted by the researcher. If the p value is greater than 0.05, the model's estimates fit the data at an acceptable level at 95% of probability. The Wald statistic tested the null hypothesis in logistic regression that a single coefficient was zero, verifying the significance of individual logistic regression coefficients for each independent variable (Norušis, 2005). In addition, the adjusted logistic model was

Table 4
Parameters and fit statistics for the logistic regression model with EWDI, elevation, and slope as predictors of red-attack damage

Model parameters		Wald test		Nagelkerke's R^2	Hosmer and Lemeshow's goodness of fit test	
Parameter	α_i	Wald	Sig.	R^2	Chi-square	Sig.
Intercept	−7.195706474	3.968	0.046	0.684	7.164	0.519
EWDI	0.104107643	11.356	0.001	$p = \frac{1}{1 + e^{-(\alpha_0 + \alpha_2 \text{EWDI} + \alpha_3 \text{Elevation} + \alpha_4 \text{Slope})}}$		
	e^{β} = 1.10971990 percent chg. in odds = 10.97					
Elevation (m)	0.006815873	11.132	0.001			
	e^{β} = 1.00683915 percent chg. in odds = 0.68					
Slope (°)	−0.170123606	8.413	0.004			
	e^{β} = −0.84356054 percent chg. in odds = −15.64					

Table 5
Results of the validation of the logistic regression model using EWDI, elevation, and slope as predictors for red-attack mapping

Predictors: EWDI, elevation, slope		Logistic model			Producer's accuracy	Omission error	
		Non-attack	Red-attack	Total			
Reference data	Non-attack	57	7	64	89.06%	10.94%	
	Red-attack	11	53	64	82.81%	17.19%	
	Total	68	60	128	Overall accuracy		
User's accuracy		83.82%	88.33%		Lower CI	Value	Upper CI
Comission error		16.18%	11.67%		78.84%	85.94%	90.89%

Confidence intervals calculated at 95% confidence coefficient.

applied to the validation dataset, and the error matrix for the binary variable (predicted versus observed) was generated, omission and commission errors were determined, and related confidence intervals calculated at 95% confidence coefficient (Czaplewski, 2003). The overall accuracy and true positive rate were also calculated. The true positive rate is the attribute specific accuracy for red-attack; this measure reports how many red-attack trees identified from the image source were actually identified in the validation data (e.g. Producer's accuracy).

4. Results

Two distinct models were developed for the area of the study site identified as lodgepole pine in the forest inventory; the first included only the EWDI values as input, using the non-attack and red-attack calibration dataset to generate a probability of red-attack damage from 0 to 1 (Fig. 6A). The parameters of this logistic regression model are provided in Table 2 and indicate that this model is weak: Nagelkerke's R^2 was 0.454; Hosmer and Lemeshow was <0.05 (model estimates do not fit the data within an acceptable level at the 95% confidence level); and the Wald statistic indicates that the EWDI was significant to the model. The odds ratio, e^{β}, and the percentage change in the odds ratio are shown in Table 2. A unit increase in EWDI, results in an increase of the odds of a pixel having red-attack damage by 17%.

For validation purposes, the cut-off value used to discriminate between attacked and non-attacked was 50%. Therefore, if a pixel had a probability of red-attack of less than 0.5, the pixel was considered non-attacked. Conversely, if the pixel had a value of greater than 0.5, the pixel was considered attacked. Using these threshold values, 44% of the forest inventory polygons had red-attack damage, accounting for 8% of the total study area, and 35% of the total area of pine forest. The results indicate a heterogeneous distribution of attack damage (Fig. 6A). The accuracy of the model output was assessed using a set of independent validation data (previously reserved from the collected ground data) (Table 3). The overall accuracy of the EWDI model was 75% with a 95% confidence interval of 67% to 82%. True positive accuracy for red-attack damage was 67%.

The second model incorporated the EWDI values with elevation, slope, and global, direct, and diffuse radiation in a logistic regression with a forward stepwise selection method. The parameters of this logistic regression model are provided in Table 4 and indicate that this model is strong; Nagelkerke's R^2 was 0.684; Hosmer and Lemeshow was >0.05 (model estimates do fit the data within an acceptable level at the 95% confidence level); and the Wald statistic indicates that the EWDI, elevation, and slope were significant to the model. None of the radiation variables were found to be significant to the classification in the forward stepwise selection process and were therefore excluded from the development of the model. The odds ratios for this model and the percentage change in the odds ratios are included in Table 4. Per unit changes in EWDI or elevation result in an increase of 11% and 0.7%, respectively, in the odds of red-attack damage. Conversely, increases in slope result in a decrease in the odds of red-attack damage by 15.64%.

The distribution of probabilities of red-attack damage appeared quite different than those from the model generated using the EWDI values only (Fig. 6B). The overall accuracy of the model output, assessed using independent validation data was 86% with 95% confidence intervals of 79% to 91% (Table 5). The true positive accuracy for red-attack detection was 83%. Using the same threshold values as for the first model (50%), the total number of forest inventory polygons with red-attack damage was 64%, accounting for 5% of the study area, and 20% of the area dominated by pine forest.

5. Discussion

The EWDI has been effectively used to detect forest disturbances (Franklin et al., 2002, 2003, 2005). The EWDI, as generated from multi-date Landsat imagery, has also been successfully used to detect and map mountain pine beetle red-attack damage at the landscape level (Coops et al., in review; Skakun et al., 2003). Areas of mixed forest are more challenging for mapping red-attack damage with a medium resolution sensor such as Landsat, since the host species has a more sparse and heterogeneous spatial distribution. In addition, areas of variable terrain present unique challenges for the classification of remotely sensed imagery, as shadows and differences in surface orientation can increase the spectral variability associated with a given cover type or target of interest.

The objective of this research was to build on experience using multi-date techniques for red-attack detection with Landsat imagery. The full distribution of EWDI values were used to estimate the probability of red-attack damage, rather than relying on the analyst's judgement to select a threshold

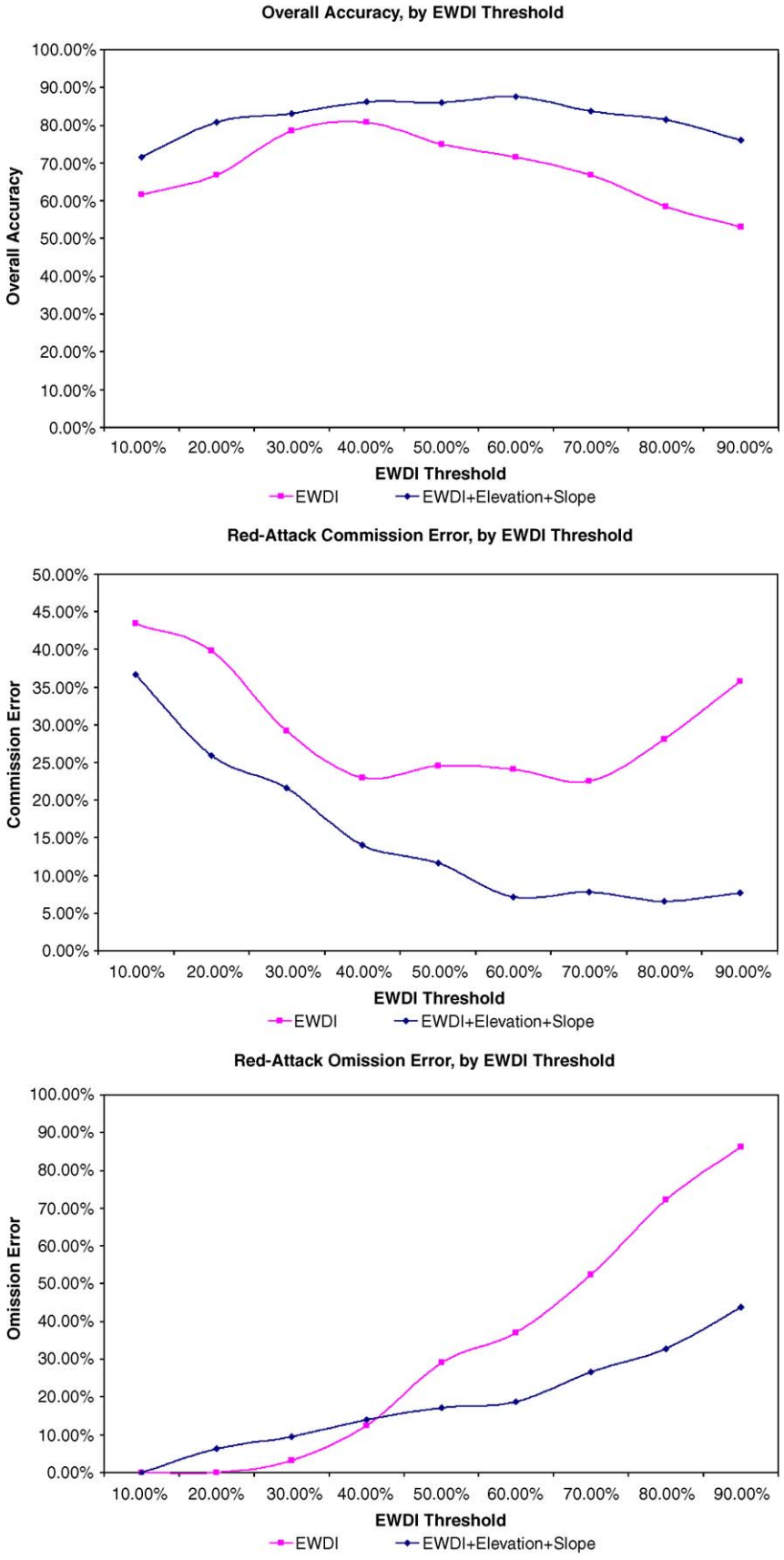

Fig. 7. Variation in overall accuracy, commission and omission errors.

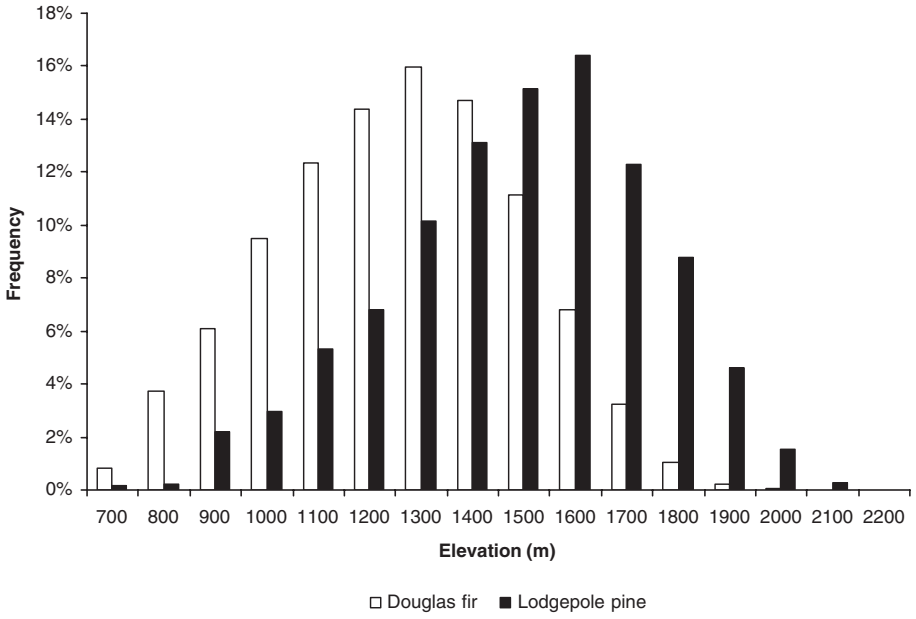

Fig. 8. Elevation distribution for lodgepole pine (*Pinus contorta*) and Douglas-fir (*Pseudotsuga menziesii*) in the study area.

based on a set of calibration samples. As Fig. 5 illustrates, there is overlap between the distributions of EWDI values for red-attack and non-attack forest stands. When a threshold for red-attack is selected, the analyst must attempt to minimize the commission error (or omission error—depending on the information need), which becomes increasingly difficult in mixed forest conditions.

A logistic regression approach was used in this study to model the probability of mountain pine beetle red-attack damage across the study area. Independent calibration samples, representing red-attack and non-attack forest stands, were input into the logistic regression model. The output from the logistic regression is a probability surface with values ranging from 0 to 1, indicating the likelihood that any given pixel has red-attack damage. Arbitrary thresholds may still be used to determine the accuracy of the classification or to produce a simple presence/absence map of red-attack damage; however, the continuous probability surface of red-attack damage offers greater flexibility from a forest management perspective. For example, with the continuous probability surface, questions such as how much of the study area had a greater than 75% likelihood of having red-attack damage (9% of the study area), how many inventory polygons contained likelihoods of greater than 75% (55% of inventory polygons) can be addressed.

Such a continuous assessment of the potential for red-attack damage across the landscape allows forest managers to provide

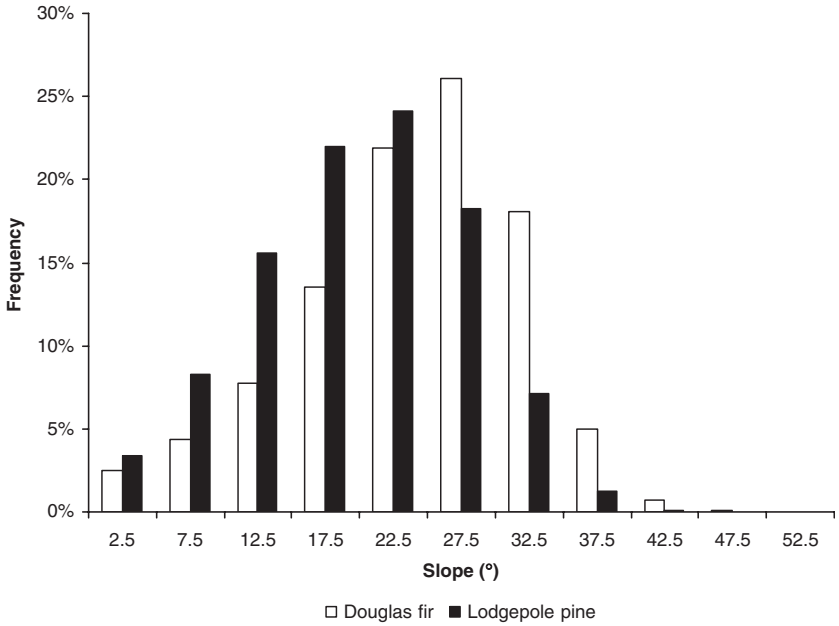

Fig. 9. Slope distribution for lodgepole pine (*Pinus contorta*) and Douglas-fir (*Pseudotsuga menziesii*) in the study area.

a flexible representation of attack damage conditions (Fig. 7). For example, forest managers may use a more stringent definition of attack when minimizing errors of commission is paramount (e.g., in an outbreak scenario, like that which is currently being experienced in western Canada and the United States). In this case, forest managers may elect to focus on those areas with a greater than 70% probability of having red-attack damage, thereby reducing the likelihood that field crews will be dispatched to locations erroneously identified as red-attack. Alternatively, a more liberal definition of damage could be considered when errors of omission are more of a concern, such as when populations of mountain pine beetle are increasing in the incipient-epidemic phase. In this case, forest managers may opt to consider all areas with a greater than 50% probability of having red-attack damage.

Another objective of this project was to incorporate elevation, slope, and solar radiation information into the red-attack mapping. To this end, these attributes were added to the logistic regression model described above. It was found that the use of elevation and slope improved the accuracy of red-attack detection, when compared to the model using EWDI values only (Tables 3 and 5). The greater accuracy achieved with this method is explained largely by the nature and distribution of the host species in the study area. The Lolo National Forest is an area of mixed forest, with a heterogeneous spatial distribution of species. In this portion of the Lolo National Forest, the elevation range is approximately 1000 m. Elevation and slope are important determinants of forest composition and structure, influencing the distribution of forest species across the landscape. Lodgepole pine, the primary host species for mountain pine beetle, are found at higher elevations in this area (Fig. 8) (e.g., along ridge tops) with relatively lower slopes (Fig. 9), when compared to the distribution of elevation and slope for Douglas-fir, the dominant species in the study area. The moisture differences between the 2 years of imagery used to generate the wetness index (1999 and 2002) were also heterogeneous, as indicated by the EWDI output in Fig. 4.

In the extreme extents of the beetle's elevational and climatic range, it can take up to 2 years for the beetle to complete its life cycle, exposing the beetle to increased predation and cold mortality. Amman (1973) found that elevation can severely restrict beetle population. It is for this reason that beetles primarily concentrate at lower elevations; however, what is considered a high or low elevation is a relative concept, in relation to latitude (Logan & Powell, 2001). Elevation and latitude/longitude affect the survival of the beetle and therefore form an important part of susceptibility models (Shore & Safranyik, 1992). Wulder et al. (2005) characterized the slope, aspect, and elevation of known red-attack locations in a 5000 km^2 study area in central British Columbia. In this particular area, with gently rolling glacial deposits and an elevation range of 600 to 800 m above sea level, slope, aspect, and elevation were not identified as key characteristics of beetle attack. In contrast, Coops et al. (in review) found that slope was an important factor in characterizing the preferential attack of mountain pine beetles in areas that had not previously supported infestations. Coops et al. (in review) examined new mountain pine beetle infestations in an area of northeastern British Columbia, with elevations ranging from 221 to 2945 m.

Solar radiation (global, direct, and diffuse) was the other variable that was considered important for predicting the likelihood of red-attack damage. It is known that mountain pine beetle prefer south facing slopes, as these areas generally receive more solar radiation and are therefore more conducive to brood survival. None of the solar radiation attributes considered were found to contribute significantly to the model, and these attributes were therefore excluded from the model in the forward stepwise selection process. The distributions of

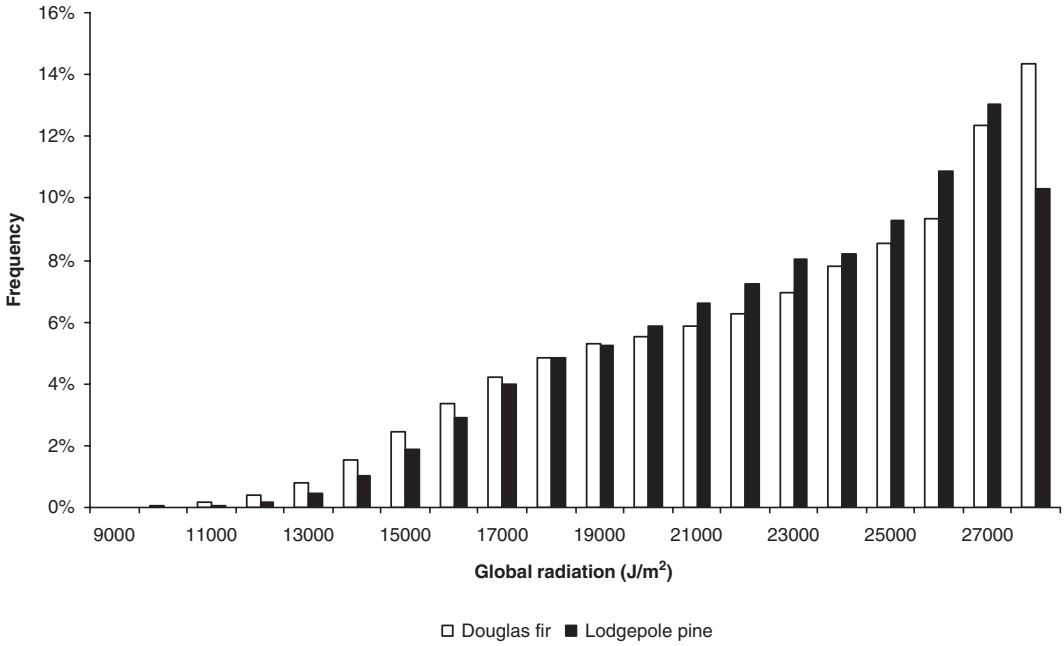

Fig. 10. Global radiation distribution for lodgepole pine (*Pinus contorta*) and Douglas-fir (*Pseudotsuga menziesii*) in the study area.

global solar radiation are similar for lodgepole pine and Douglas-fir, and this may explain the lack of discriminating power of these variables (Fig. 10).

The aerial overview survey data, presented in Fig. 2, indicates broad areas of red-attack damage. The differences in the representation of red-attack damage between the overview surveys and the temporal sequence of Landsat imagery methods have been documented (Wulder et al., 2005); approaches using remotely sensed data are more spatially explicit, while the aerial overview survey often incorporates large areas of non-attack in its estimates of damage. However, a comparison of the overview survey with

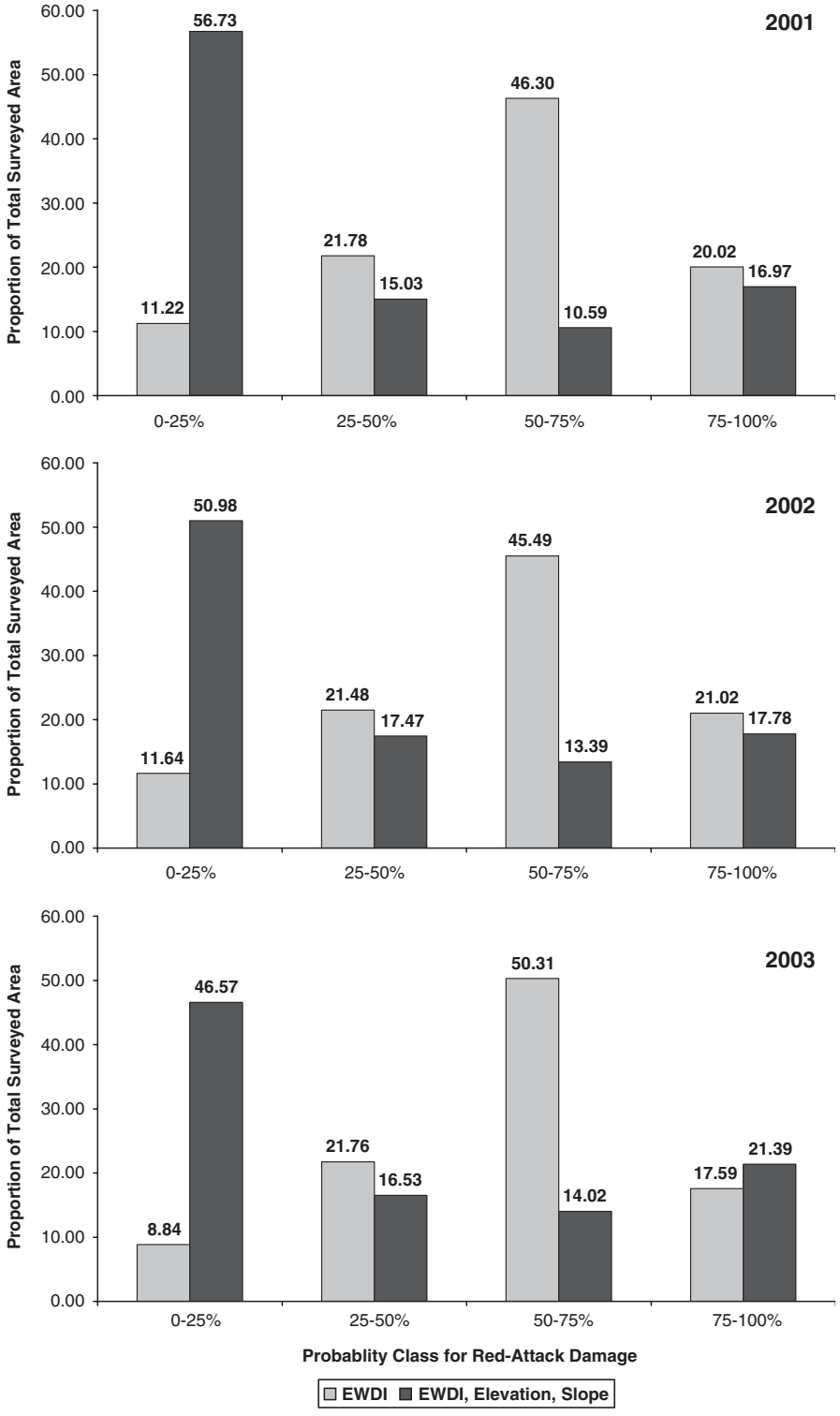

Fig. 11. Distribution of red-attack probabilities within areas of red-attack identified in 2001, 2002, and 2003 aerial overview survey data.

the probabilities generated from the Landsat temporal sequence in this study provides some insights on how the two logistic regression models are functioning. The distribution of red-attack probabilities (grouped into four classes, in 25% increments), by the year of the overview survey, is provided in Fig. 11. Both logistic regression models are very similar in the 25% to 50% and in the 75% to 100% likelihood range, with 15% to 20% of the surveyed area in 2001, 2002, and 2003 found in these two likelihood categories. Where these models differ markedly is in the 0% to 25% and 50% to 75% likelihood classes. Here, the model that incorporates the EWDI, elevation, and slope assigns more of the surveyed area to a lower likelihood of attack class. Conversely, the model generated using only the EWDI values assigns more of the surveyed area to a higher likelihood of attack class. This comparison illustrates how the addition of ancillary variables relevant to the stand conditions in the study area can help to improve the accuracy of the red-attack damage estimates.

6. Conclusion

As a result of the mixed forest conditions and variable terrain in the study area, the logistic regression model that incorporated moisture differences (EWDI), elevation, and slope, more accurately predicted the likelihood of red-attack damage, by a margin of 11% over the model that used moisture differences alone. Solar radiation, in various forms (direct, diffuse, and global), did not contribute any significant improvement to model performance and was excluded.

The results of this study have several implications for the use of satellite imagery to map mountain pine beetle red-attack damage at the landscape level. The first is the generation of a continuous probability surface to represent the likelihood of red-attack damage, rather than the use of an arbitrary threshold of EWDI values to identify red-attack locations. This probability surface provides forest managers with greater flexibility in assessing and responding to a widespread mountain pine beetle infestation.

The additional implication of these results is the demonstrated utility of including other ancillary variables in the determination of red-attack likelihood. The use of elevation and slope in conjunction with the EWDI values produced a more accurate representation of the likelihood of red-attack damage than the model that relied solely on the EWDI values. These results suggest that the accuracy of red-attack detection with Landsat imagery can be improved by use of these additional variables in areas where the conditions are suitable (e.g., mixed forests, variable terrain).

Landsat data, and data from other remote sensing satellites with similar spatial and spectral resolutions, provide a valuable source of information regarding the location and extent of mountain pine beetle infestations. These medium resolution sensors afford the synoptic and spatially explicit identification of red-attack damage at the landscape level, and thereby form an important component of a larger data hierarchy that relies on this cost-effective and coarser data to guide the acquisition of more expensive and higher resolution data sources.

Acknowledgements

Elements of this project were funded by the Government of Canada through the Mountain Pine Beetle Initiative, a 6-year, $40 million program administered by Natural Resources Canada, Canadian Forest Service (http://mpb.cfs.nrcan.gc.ca). David Seemann and Danny Grills of the Canadian Forest Service are thanked for their assistance with image pre-processing and figure production. Daniel Endreson and Leslie Brown assisted with ground data collection and image acquisition and initial processing. Jim Vandygriff, Matt Hansen, Rebecca Gerhardt, and Amy Adams also assisted with ground data collection. The USDA Forest Service, Special Technology Development Program provided partial funding for ground data collection and image acquisition and analysis. M. Flor Alvarez Taboada received support from the Fundación Caixa Galicia (a Postgraduate Grant enabling a residency at the Pacific Forestry Centre (Victoria) of the Canadian Forest Service).

References

Amman, G. D. (1973). Population changes of the mountain pine beetle in relation to elevation. *Environmental Entomology*, *2*, 541–547.

Amman, G. D. (1982). Characteristics of mountain pine beetles reared in four pine hosts. *Environmental Entomology*, *11*, 590–593.

Amman, G. W., & Cole, W. E. (1983). Mountain pine beetle dynamics in lodgepole pine forests part II: Population dynamics. *Technical Report. INT-145* (p. 59). USDA For. Serv. Gen.

Amman, G. D., Thier, R. W., McGregor, M. D., & Schmitz, R. F. (1989). Efficacy of verbenone in reducing lodgepole pine infestation by mountain pine beetles in Idaho. *Canadian Journal of Forest Research*, *19*, 60–64.

Ardö, J., Pilesjö, P., & Skidmore, A. (1997). Neural networks, multitemporal Landsat Thematic Mapper data and topographic data to classify forest damages in the Czech Republic. *Canadian Journal of Remote Sensing*, *23*, 217–229.

Ballard, R. G., Walsh, M. A., & Cole, W. E. (1982). Blue-stain fungi in xylem of lodgepole pine: A light microscope study on extent of hyphal distribution. *Canadian Journal of Botany*, *60*, 2334–2341.

Ballard, R. G., Walsh, M. A., & Cole, W. E. (1984). The penetration and growth of blue-stain fungi in the sapwood of lodgepole pine attacked by mountain pine beetle. *Canadian Journal of Botany*, *62*, 1724–1729.

Bergerud, W. A., 1996. *Introduction to logistic regression models with worked forestry examples: biometrics information handbook no.7.* Res. Br., British Columbia Ministry of Forests, Victoria, B.C. Working Paper. 157 pp.

Berryman, A. A. (1976). Theoretical explanation of mountain pine beetle dynamics in lodgepole pine forests. *Environmental Entomology*, *5*, 1225–1233.

Berryman, A. A., Raffa, K. F., Millstein, J. A., & Stenseth, N. C. (1989). Interaction dynamics of bark beetle aggregation and conifer defense rates. *Oikos*, *56*, 256–263.

British Columbia Ministry of Forests. (1995). Bark beetle management guidebook. *Forest practices code*. Victoria, BC: Forest Practices Branch. 45 pp.

Burrough, P. A. (1986). *Principles of geographical information systems for land resources assessment*. Oxford: Clarendon Press. 193 pp.

Carroll, A. L., & Safranyik, L. (2004). The bionomics of the mountain pine beetle in lodgepole pine forests: Establishing a context. In T. L. Shore, J. E. Brooks, & J. E. Stone (Eds.), *Mountain pine beetle symposium: Challenges*

and solutions (pp. 21–32). Victoria, Canada: Pacific Forestry Centre, Natural Resources Canada.

Carroll, A. L., Taylor, S. W., Régnière, J., & Safranyik, L. (2004). Effects of climate change on range expansion by the mountain pine beetle in British Columbia. In T. L. Shore, J. E. Brooks, & J. E. Stone (Eds.), *Mountain pine beetle symposium: Challenges and solutions* (pp. 223–232). Victoria, Canada: Pacific Forestry Centre, Natural Resources Canada.

Cohen, W. A., Maiersperger, T. K., Gower, S. T., & Turner, D. P. (2003). An improved strategy for regression of biophysical variables and Landsat ETM+ data. *Remote Sensing of Environment*, *84*, 561–571.

Cohen, W. B., Spies, T. A., & Fiorella, M. (1995). Estimating the age and structure of forests in a multi-ownership landscape of Western Oregon, U.S.A.. *International Journal of Remote Sensing*, *16*, 721–746.

Collins, J. B., & Woodcock, C. E. (1996). An assessment of several linear change detection techniques for mapping forest mortality using multitemporal Landsat TM data. *Remote Sensing of Environment*, *26*, 66–77.

Coops, N., Wulder, M., & White, J. C. (in review). Characterizing preferential attack by mountain pine beetle in susceptible forest stands, *Forest Ecology and Management* (submitted June 15, 2005).

Crist, E. P., & Cicone, R. C. (1984). Application of the tasseled cap concept to simulated Thematic Mapper data. *Photogrammetric Engineering and Remote Sensing*, *50*, 327–331.

Crist, E. P., & Kauth, R. J. (1986). The tasseled cap demystified. *Photogrammetric Engineering and Remote Sensing*, *51*, 1315–1330.

Crist, E. P., Lauren, R., & Cicone, R. C. (1986). *Vegetation and soils information contained in transformed Thematic Mapper data*. Final Proceedings: IGARSS '86 Symposium. Zurich, Switzerland, 8–11 September. Noordwijk, The Netherlands: ESA Publ. Division.

Czaplewski, R. L. (2003). Accuracy assessment of maps of forest condition. In M. A. Wulder, & S. E. Franklin (Eds.), *Remote sensing of forest environments: Concepts and case studies* (pp. 115–140). Boston: Kluwer Academic Publishers.

Dymond, C. C., Mladenoff, D. J., & Radeloff, V. C. (2002). Phenological differences in tasseled cap indices improve deciduous forest classification. *Remote Sensing of Environment*, *80*, 460–472.

Franklin, J. (1995). Predictive vegetation mapping: Geographic modelling of biospatial patterns in relation to environmental gradients. *Progress in Physical Geography*, *19*, 474–499.

Franklin, S. E., Jagielko, C. B., & Lavigne, M. B. (2005). Sensitivity of the Landsat enhanced wetness difference index (EWDI) to temporal resolution. *Canadian Journal of Remote Sensing*, *31*, 149–152.

Franklin, S. E., Lavigne, M., Wulder, M. A., & Stenhouse, G. B. (2002). Change detection and landscape structure mapping using remote sensing. *The Forestry Chronicle*, *78*, 618–625.

Franklin, S. E., Lavigne, M. B., Moskal, L. M., Wulder, M. A., & McCaffrey, T. M. (2001). Interpretation of forest harvest conditions in New Brunswick using Landsat TM enhanced wetness difference imagery (EWDI). *Canadian Journal of Remote Sensing*, *27*, 118–128.

Franklin, S. E., Moskal, L. M., Lavigne, M., & Pugh, K. (2000). Interpretation and classification of partially harvested forest stands in the Fundy model forest using multitemporal Landsat TM digital data. *Canadian Journal of Remote Sensing*, *26*, 318–333.

Franklin, S. E., Wulder, M. A., Skakun, R., & Carroll, A. (2003). Mountain pine beetle red-attack forest damage classification using stratified Landsat TM data in British Columbia, Canada. *Photogrammetric Engineering and Remote Sensing*, *69*, 283–288.

Fraser, R. H., Abuelgasim, T. A., & Latifovic, R. (2005). A method for detecting large-scale forest cover change using coarse spatial resolution imagery. *Remote Sensing of Environment*, *95*, 414–427.

Fraser, R. H., Fernandes, R., & Latifovic, R. (2003). Multi-temporal mapping of burned forest over Canada using satellite-based change metrics. *Geocarto International*, *18*, 37–47.

Fraser, R. H., & Latifovic, R. (2005). Mapping insect-induced tree defoliation and mortality using coarse spatial resolution satellite imagery. *International Journal of Remote Sensing*, *26*, 193–200.

Furniss, M. M., & Schenk, J. A. (1969). Sustained natural infestation by the mountain pine beetle in seven new *Pinus* and *Picea* hosts. *Journal of Economic Entomology*, *62*, 518–519.

Gong, P., Mahler, S. A., Biging, G. S., & Newburn, D. A. (2003). Vineyard identification in an oak woodland landscape with airborne digital camera imagery. *International Journal of Remote Sensing*, *24*, 1303–1315.

Healy, S. P., Cohen, W. B., Zhiqiang, Y., & Krankina, O. N. (2005). Comparison of tasseled cap-based Landsat data structures for use in forest disturbance detection. *Remote Sensing of Environment*, *97*, 301–310.

Henigman, J., Ebata, T., Allen, E., & Pollard, A. (Eds.). (1999). *Field guide to forest damage in British Columbia*. Victoria, BC: British Columbia Ministry of Forests.

Hill, J. B., Poop, H. W., & Grove Jr., A. R. (1967). *Botany: A textbook for colleges* (4th edition). Toronto, ON: McGraw-Hill Book Co. 614 pp.

Horler, D. N. H., & Ahern, F. J. (1986). Forestry information content of Thematic Mapper data. *International Journal of Remote Sensing*, *7*, 405–428.

Hosmer, D. W., & Lemeshow, S. (2000). Applied logistic regression. *Wiley series in probability and statistics*. New York: Wiley-Interscience. 392 pp.

Huang, C., Wylie, B., Yang, L., Homer, C., & Zylstra, G. (2002). Derivation of a tasselled cap transformation based on Landsat 7 at-satellite reflectance. *International Journal of Remote Sensing*, *23*, 1741–1748.

Kauth, R. J., & Thomas, G. S. (1976). The tasseled cap–a graphic description of spectral–temporal development of agricultural crops as seen by Landsat. *Final proceedings: 2nd international symposium on machine processing of remotely sensed data*. West Lafayette, IN: Purdue University.

Kreith, F., & Kreider, J. F. (1978). *Principles of solar engineering*. New York: McGraw-Hill.

Kumar, L., Skidmore, A. K., & Knowles, E. (1997). Modelling topographic variation in solar radiation in a GIS environment. *International Journal for Geographical Information Science*, *11*, 475–497.

Lambert, N. J., Ardö, J., Rock, B. N., & Vogelmann, J. E. (1995). Spectral Characterization and regression based classification of forest damage in Norway spruce Stands in the Czech Republic using Landsat TM data. *International Journal of Remote Sensing*, *16*, 1261–1287.

Logan, J. A., & Bentz, B. J. (1999). Model analysis of mountain pine beetle (Coleptera: Scolytidae) seasonality. *Environmental Entomology*, *28*, 924–934.

Logan, J. A., & Powell, J. A. (2001). Ghost forests, global warming, and the mountain pine beetle (Coleoptera: Scolytidae). *American Entomologist*, *47*, 160–172.

Logan, J. A, & Powell, J. A. (2004). Modelling mountain pine beetle phenological response to temperature. In T. L. Shore, J. E. Brooks, & J. E. Stone (Eds.), *Mountain pine beetle symposium: Challenges and solutions*. *Information Report BC-X-399.* Victoria, BC, Canada: Pacific Forestry Centre. 298 pp.

Magnussen, S., Boudewyn, P., & Alfaro, R. (2004). Spatial prediction of the onset of spruce budworm defoliation. *The Forestry Chronicle*, *80*, 485–494.

Markham, B., & Barker, J. (1986). Landsat MSS and TM post calibration dynamic ranges, exoatmospheric reflectances and at satelite temperature. *EOSAT Landsat Technical Notes*, *1*, 3–7.

Mathre, D. E. (1964). Pathogenicity of *Ceratocystis ips* and *Ceratocystis minor* to *Pinus ponderosa*. *Contribution Boyce Thompson Institute*, *22*, 363–388.

Monserud, R. A. (1976). Simulation of forest mortality. *Forest Science*, *22*, 438–444.

Monserud, R. A., & Sterba, H. (1999). Modeling individual tree mortality for Austrian forest species. *Forest Ecology and Management*, *113*, 109–123.

Nagelkerke, N. J. D. (1991). A note on a general definition of the coefficient of determination. *Biometrika*, *78*, 691–692.

Norušis, M. J. (2005). *SPSS 13.0 advanced statistical procedures*. Prentice Hall. 368 pp.

Oksanen, J., & Sarjakoski, T. (2005). Error propagation of DEM-based surface derivatives. *Computers & Geosciences*, *31*, 1015–1027.

Peduzzi, P., Concato, J., Kemper, E., Holford, T. R., & Feinstein, A. (1996). A simulation of the number of events per variable in logistic regression analysis. *Journal of Clinical Epidemiology*, *99*, 1373–1379.

Press, S. J., & Wilson, S. (1978). Choosing between logistic regression and discriminant analysis. *Journal of the American Statistical Association*, *73*, 699–705.

Price, K. P., & Jakubauskas, M. E. (1998). Spectral retrogression and insect damage in lodgepole pine successional forests. *International Journal of Remote Sensing.*, *19*, 1627–1632.

Raffa, K. F., & Berryman, A. A. (1983). Physiological aspects of lodgepole pine wound responses to a fungal symbiont of the mountain pine beetle, *Dendroctonus ponderosae* (Coleoptera: Scolytidae). *Canadian Entomologist*, *115*, 723–734.

Reid, R. W. (1961). Moisture changes in lodgepole pine before and after attack by the mountain pine beetle. *Forestry Chronicle*, 368–375.

Rice, J. C. (1994). Logistic regression: An introduction. In B. Thompson (Ed.), *Advances in social science methodology*, *vol. 3* (pp. 191–245). Greenwich, CT: JAI Press.

Safranyik, L. (1978). Effects of climate and weather on mountain pine beetle populations. In D. L. Kibbee, A. A. Berryman, G. D. Amman, & R. W. Stark (Eds.), *Theory and practice of mountain pine beetle management in lodgepole pine forests* (pp. 79–86). Idaho, Moscow, ID: Symp. Proc. Univ.

Safranyik, L. (2004). Mountain pine beetle epidemiology in lodgepole pine. In Shore, T. L. Brooks, J. E., & Stone, J. E. (Eds.), *Mountain Pine Beetle symposium: Challenges and solutions, October 30–31, 2003, Kelowna, British Columbia, Canada.* Natural Resources Canada, Canadian Forest Service, Pacific Forestry Centre, Victoria, British Columbia, Information Report BC-X-399. 298 pp.

Safranyik, L., Shrimpton, D. M., & Whitney, H. S. (1974). *Management of lodgepole pine to reduce losses from the mountain pine beetle*. Government of Canada. Department of the Environment. Canadian Forest Service, Pacific Forest Research Centre, Victoria, BC. Forestry Technical Report 1.

Safranyik, L., Shrimpton, D. M., & Whitney, H. S. (1975). An interpretation of the interaction between lodgepole pine, the mountain pine beetle, and its associated blue stain fungi in western Canada. In D. M. Baumgartner (Ed.), *Management of lodgepole pine ecosystems* (pp. 406–428). Pullman, WA: Washington State University Cooperative Extension Service.

Shen, G., Moore, J. A., & Hatch, C. R. (2000). The effect of nitrogen fertilization, rock type, and habitat type on individual tree mortality. *Forest Science*, *47*, 203–213.

Shore, T., & Safranyik, L. (1992). Susceptibility and risk rating systems for the mountain pine beetle in lodgepole pine stands. Forestry Canada, Pacific and Yukon Region, Pacific Forestry Centre, Victoria, British Columbia, Information Report BC-X-336. 12 pp.

Skakun, R. S., Wulder, M. A., & Franklin, S. E. (2003). Sensitivity of the thematic mapper enhanced wetness difference index to detect mountain pine beetle red-attack damage. *Remote Sensing of Environment*, *86*, 433–443.

Smith, R. H., Wickman, B. E., Hall, R. C., DeMars, C. J., & Ferrell, G. T. (1981). The California pine risk-rating system: Its development, use, and relationship to other systems. In R.L. Hedden, S.J. Barras, & J.E. Coster (Tech. Coords), *Proceedings of the Symposium on Hazard-rating Systems in Forest Pest Management, July 31–August 1, 1980, Athens, GA* (pp. 53–69). USDA For. Serv. Gen. Tech. Rep. WO-27.

Solheim, H. (1995). Early stages of blue-stain fungus invasion of lodgepole pine sapwood following mountain pine beetle attack. *Canadian Journal of Botany*, *73*, 70–74.

Taylor, S. W. & Carroll, A. L. (2004) Disturbance, forest age, and mountain pine beetle outbreak dynamics in BC: A historical perspective. In T. L. Shore, J. E. Brooks, & J. E. Stone, (Eds.), *Mountain Pine Beetle symposium: Challenges and solutions, October 30–31, 2003, Kelowna, British Columbia, Canada.* Natural Resources Canada, Canadian Forest Service, Pacific Forestry Centre, Victoria, British Columbia, Information Report BC-X-399. 298 pp.

United States Geological Survey (USGS). (1999). National Elevation Dataset, EROS Data Center, Edition 1. http://csd.unl.edu/general/nedsmetadata.asp. Accessed August 15, 2005.

Vanclay, J. K. (1995). Growth models for tropical forests: a synthesis of models and methods. *Forest Science*, *41*, 7–42.

Westfall, J. (2005). *2004 Summary of forest health conditions in British Columbia*. Forest Practices Branch, Victoria, BC: British Columbia Ministry of Forests. 49 pp.

Wulder, M. A., Dymond, C. C., & Erickson, B. (2004). *Detection and monitoring of the mountain pine beetle*. Forest Practices Branch, Victoria, BC: Canadian Forest Service, Pacific Forestry Centre, Victoria, British Columbia BC-X-398.

Wulder, M. A., Skakun, R. S., Franklin, S. E., & White, J. C. (2005). Enhancing forest inventories with mountain pine beetle infestation information. *Forestry Chronicle*, *81*, 149–159.

Yamaoka, Y., Swanson, R. H., & Hiratsuka, Y. (1990). Inoculation of lodgepole pine with four blue-stain fungi associated with mountain pine beetle, monitored by a Heat Pulse Velocity (HPV) instrument. *Canadian Journal of Forest Research*, *20*, 31–36.

Yao, X., Titus, S., & MacDonald, S. E. (2001). A generalized logistic model of individual tree mortality for aspen, white spruce, and lodgepole pine in Alberta mixedwood forests. *Canadian Journal of Forest Research*, *31*, 283–291.